TABLE 1 Injection-Locked Frequency Divider Comparison

Ref.	P_{in} (dBm)	Supply Voltage (v)	P_{diss} (mw)	Die Area (mm^2)	Locking-Range (GHz)
This work	0	1	2.6	0.48	3.84–5.12
4	600 mV	1.5	1.2	0.7	3.1–3.5
5	4	2.5	16.8	0.35	38.3–40.6
2	7	1.5	23	0.21	14.2–17.2
1	0	0.75	4.5	0.65	3.27–4.64

noise. Figure 8 shows the measured phase noises of the free-running, injection signal and injection-locked oscillator outputs in the divide-by-2 mode. The phase noise of free-running oscillator at 1 MHz offset is about −113 dBc/Hz. After external power injection at 0 dBm, the ILFD phase noise is about −134 dBc/Hz in the divide-by-2 mode. The phase noise of divide-by-2 ILFD is lower than that of the free-running oscillator by 21 dB.

Table 1 shows the comparison between our presented injection-locked divider and previously published reports. The FD has a comparable performance but with the smaller occupied chip area.

4. CONCLUSION

A small die area 2.4-GHz FD employing the 3D helical inductors fabricated in the 0.18-μm CMOS technology have been demonstrated, and the FD circuit uses the concept of inductor tapping to shift the parasitic drain-to-bulk junction capacitances of active switching MOSFET's away from paralleling with the varactors. The fixed capacitance that affects the tuning range is reduced; therefore, the locking range can be increased. Two 3D inductors have been used to reduce the chip occupied area and lower chip cost. The die area is 0.664×0.731 mm^2. The same concept of using single 3D inductor in FD can be used to reduce chip size of FD with an inductor. The implemented FD core consumes power of 2.6 mW at 1 V supply voltage, and the measured locked phase noise is −134 dBc/Hz at 1 MHz offset from the output oscillation frequency of 2.34 GHz.

ACKNOWLEDGMENT

The authors thank the Staff of the CIC for the chip fabrication and technical supports.

REFERENCES

1. Y.-H. Chuang, S.-H. Lee, R.-H. Yen, S.-L. Jang, J.-F. Lee, and M.-H. Juang, A wide locking range and low voltage CMOS direct injection-locked frequency divider, IEEE Microwave Wireless Compon Lett 16 (2006), 299–301.
2. M. Tiebout, A CMOS direct injection-locked oscillator topology as high-frequency low-power frequency divider, IEEE J Solid State Circuits 39 (2004), 1170–1174.
3. J. Gil, S.-S. Song, H. Lee, and H. Shin, A −119.2 dBc/Hz at 1 MHz, 1.5 mW, fully integrated, 2.5-GHz, CMOS VCO using helical inductors, IEEE Microwave Wireless Compon Lett 13 (2003), 457–459.
4. S.-H. Lee, Y.-H. Chuang, L.-R. Chi, S.-L. Jang, and J.-F. Lee, A low-voltage 2.4 GHz VCO with 3D helical inductors, In: IEEE APCCS, Singapore, 2006.
5. H.R. Rategh and T.H. Lee, Superharmonic injection-locked frequency dividers, IEEE J Solid-State Circuits 34 (1999), 813–821.

GAP COUPLED RECTANGULAR MICROSTRIP ANTENNAS FOR DUAL AND TRIPLE FREQUENCY OPERATION

K. P. Ray,[1] V. Sevani,[2] and R. K. Kulkarni[2]
[1] SAMEER, IIT Campus, Powai, Mumbai 400076, India
[2] VESIT, Chembur, Mumbai 400071, India

Received 17 October 2006

ABSTRACT: *A rectangular microstrip antenna is gradually divided into equal smaller elements along the width, and lengths of these smaller strips are varied to increase the separation between the resonances to obtain dual and triple frequency operation. Likewise, configurations consisting a maximum of five strips have been investigated. For configurations with two strips only dual frequency operation has been obtained, whereas for configurations with more than two strips both dual and triple frequency operation has been obtained. With increase in number of elements, the separation between different resonances is more and the radiation pattern is also similar in two frequency bands. Experiments have been performed and the results are in agreement with the simulations.* © 2007 Wiley Periodicals, Inc. Microwave Opt Technol Lett 49: 1480–1486, 2007; Published online in Wiley InterScience (www.interscience.wiley.com). DOI 10.1002/mop.22452

Key words: *gap coupled rectangular microstrip antenna; dual frequency rectangular microstrip antenna; triple frequency microstrip antennas; compact gap coupled microstrip antennas*

1. INTRODUCTION

Full sizes as well as shorted microstrip antennas (MSAs) are coupled with each other to achieve broadband and dual/triple frequency operations [1–3]. These configurations occupy relatively large area. To overcome this problem, a compact gap coupled rectangular microstrip antenna (RMSA) is realized by splitting it into smaller strips. The resonance frequency of a RMSA primarily depends on it's length. Therefore, if a RMSA is divided into smaller elements along the width keeping the length same, these smaller elements radiate at almost same frequency as the original RMSA leading to increase in bandwidth [4]. Also, the number of resonances increases as the number of elements increases. By increasing the separation between the resonances, by appropriately varying the length leading to variation of resonance frequency of the smaller elements, it is possible to obtain dual or triple frequency operation.

Dual and triple frequency operation obtained by equally splitting an RMSA into smaller elements along the width, has been investigated in detail in this article. An RMSA is equally splitted into smaller elements along the width, keeping the length same. Of these smaller elements, one of the elements is coaxially fed while others are gap coupled to it's nonradiating edges. Then, the lengths of the individual elements are varied so as to sufficiently increase the separation between the resonances to obtain satisfactory dual or triple frequency operation. The

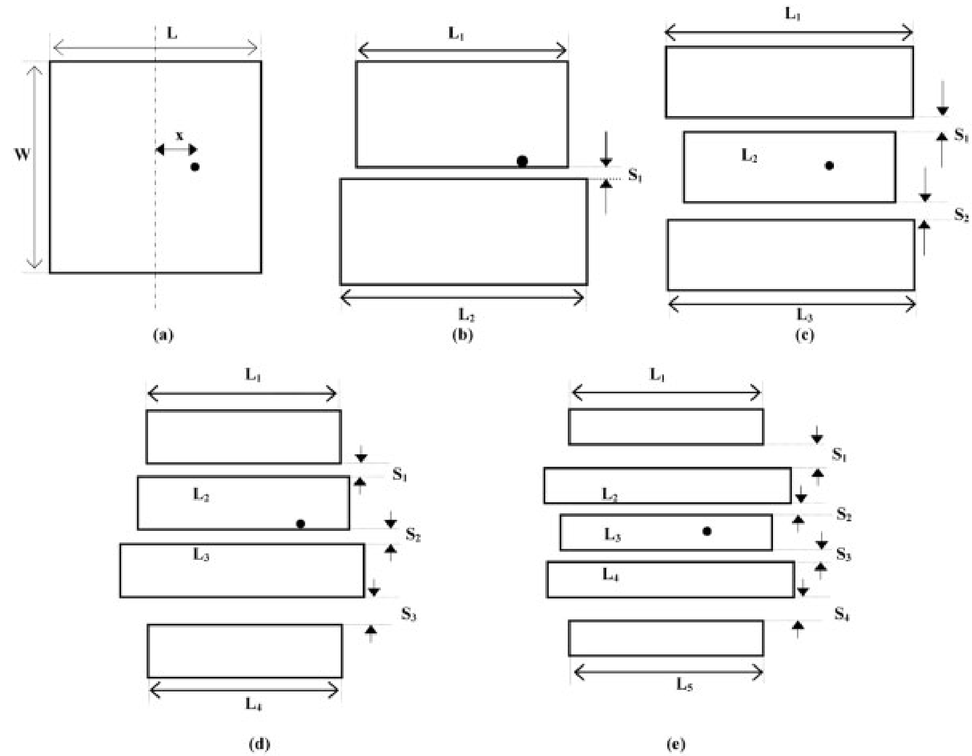

Figure 1 Gap coupled RMSA configurations obtained by splitting a single RMSA into smaller elements along the width; (a) single RMSA, Gap-coupled configuration with (b) two strips, (c) three strips, (d) four strips, and (e) five strips

RMSA is splitted into a maximum number of five smaller strips, and the performance of each configuration has been investigated in detail. For configuration with two strips, as there are only two resonating elements in the system, only dual frequency operation has been obtained; but for configuration with more than two strips both dual and triple frequency operations have been achieved. Simulations have been carried out using commercially available MoM software, IE3D [5].

2. DUAL AND TRIPLE FREQUENCY OPERATION USING GAP COUPLED RMSA STRIPS

First, a single RMSA is designed to operate at 2 GHz. The substrate parameters chosen are $\varepsilon_r = 4.3$, $h = 1.59$ mm, and tan $\delta = 0.02$. The formulas given in Ref. 3 are followed and the calculated parameters are, length $L = 35$ mm and width $W = 46.07$ mm. A bandwidth of 48 MHz is obtained when the patch is fed at $x = 8.9$ mm, using N type coaxial connector with diameter, $d = 3$ mm.

2.1. Configuration with Two Strips for Dual Band Operation

The single RMSA as mentioned earlier, is then equally splitted into two smaller elements along the width keeping the length same. Of these smaller elements, one of the element is fed using coaxial probe, while other is gap coupled to it's nonradiating edge as shown in Figure 1(b). Now, since two elements are radiating in the system, two closely spaced resonances are obtained, and a loop is observed in the impedance loci on the Smith Chart. The size of the loop depends on the coupling gap, while it's position on the Smith Chart depends on the feed point [3, 6, 7]. If the feed point is moved away from center towards the edge, then the loop shifts to right, i.e., towards high resistance region on the Smith Chart. By properly adjusting the gap and feed point, both broadband and dual frequency operation are possible for this configuration [3, 4]. The feed point and gap are properly adjusted so that satisfactory dual frequency operation is obtained for this configuration with maximum bandwidth in two frequency bands. For a gap $S = 0.5$ mm, length of both the patches as 35 mm and feed point $x = 8.2$ mm, dual frequency operation is obtained with two resonance frequencies being 2.01 and 2.117 GHz, with a frequency ratio of 1.05, as can be seen from Table 1. Reasonably good bandwidths in two frequency bands are obtained.

If the resonance frequency of one of the element is varied, then the separation between two resonances can be further increased, yielding larger frequency ratio. The resonance frequency of the parasitic element has been varied by changing it's length. The length of one of the element is kept same as the original element, i.e., 35 mm, while the length of the other element is varied from smallest to largest. It is observed that if the difference between the lengths of the two elements is large, then the separation between two resonances is also more yielding higher frequency ratio, but it becomes difficult to provide proper matching at both the frequencies and so bandwidths at individual frequency bands are small. Also, it has been observed that the response of the configuration is different when bigger strip is fed than when smaller strip is fed. When smaller strip is fed, it is observed that the loop in the impedance loci gets formed at lower frequency, which is because the parasitic patch has bigger length. A loop in the higher frequency range gets formed when bigger patch is fed, as is seen from Figure 2. Figure 2 shows the impedance loci and corresponding return loss for both these cases by feeding both bigger and smaller patch, while Table 1 summarizes the performance of this configuration for different lengths. It is seen that the range of lengths that yielded dual frequency operation with good matching at both the frequencies is 33.5–36.5 mm and the maximum frequency ratio that is obtained is 1.07.

TABLE 1 Dual Frequency Response of Configuration with Two Strips

L_1 (fed patch) (mm)	L_2 (mm)	S (mm)	x (mm)	f_{r1} (GHz)	RL_1 (dB)	BW_1 (MHz)	f_{r2} (GHz)	RL_2 (dB)	BW_2 (MHz)	f_{r2}/f_{r1}
35	33.5	0.5	9.7	2.034	−10.81	38	2.172	−11.17	20	1.07
33.5	35	—	—	—	—	—	—	—	—	—
35	34	0.5	9.7	2.031	−12.43	52	2.146	−17.67	37	1.06
34	35	0.5	8.2	2.027	−11.51	26	2.154	−10.84	27	1.06
35	35	0.5	8.2	2.01	−22.9	52	2.117	−20.03	41	1.05
36	35	0.5	9.7	1.977	−12.74	50	2.087	−17.07	36	1.06
35	36	0.5	8.2	1.973	−11.13	22	2.099	−11.7	30	1.06
36.5	35	0.5	9.7	1.955	−11.35	39	2.084	−11.03	18	1.07
35	36.5	—	—	—	—	—	—	—	—	—

$\varepsilon_r = 4.3$, $h = 1.59$ mm, $\tan \delta = 0.02$, $W = 23.04$ mm.

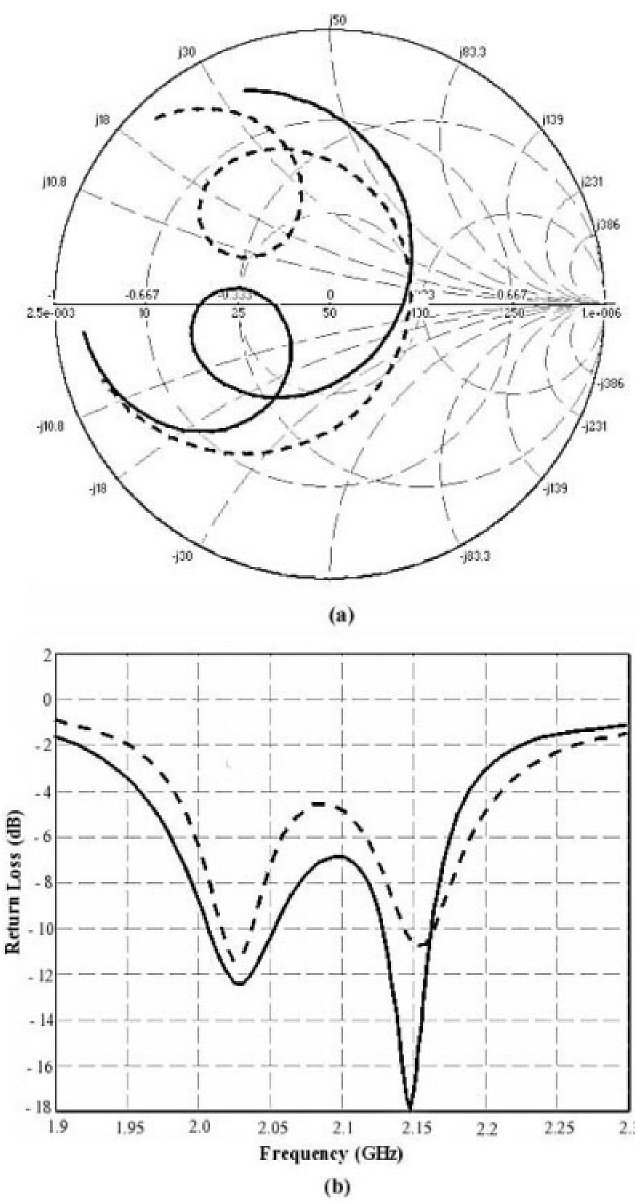

Figure 2 (a) Input impedance loci, (b) return loss plot for dual frequency operation of two strip configuration with lengths of two strips as 35 and 34 mm, by feeding both bigger and smaller strip, (——) bigger strip fed, (- - -) smaller strip fed

Figure 3 shows the radiation pattern for one of these configurations with the lengths of two elements being 35 and 34 mm, with bigger strip fed. Radiation pattern at first frequency, is in the broadside direction in both the planes, however at second frequency band, it is in broadside direction in *E*-plane, but in *H*-plane it has slight shift away from broadside. This is because at second frequency band, radiation due to parasitic element is more dominant, and as the configuration is asymmetrical with respect to the feed point, it experiences phase delay and so beam maxima shifts away slightly from broadside as can be seen from Figure 3. It is seen that at second frequency band, in *H*-plane, the beam maxima shifts to −25° from broadside, however level is only 1.5 dB less at

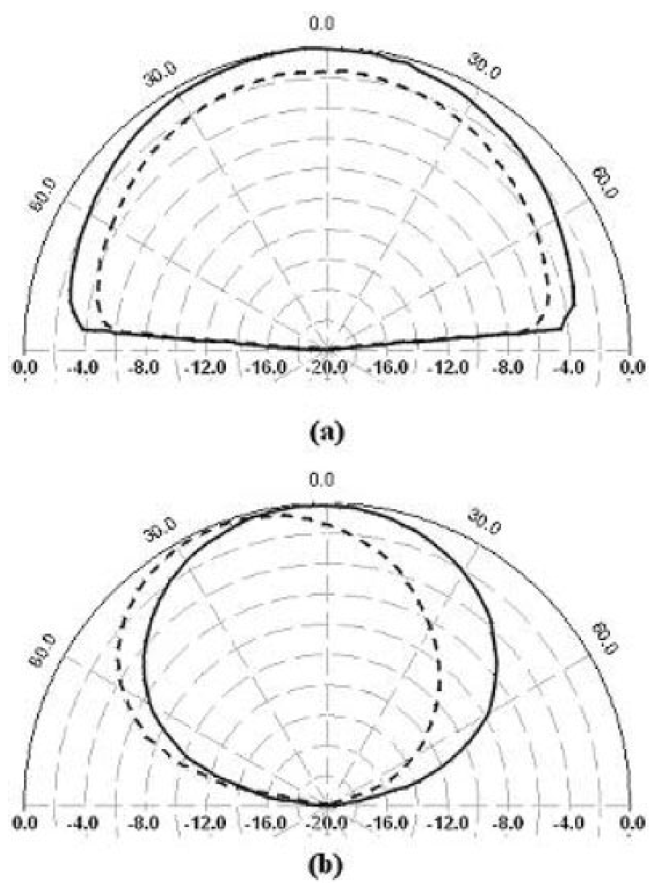

Figure 3 Radiation pattern of two strip dual band configuration with lengths of two strips as 35 and 34 mm at two frequencies with larger strip fed, (——) lower frequency, (- - -) upper frequency in (a) *E*-plane, (b) *H*-plane

TABLE 2 Dual and Triple Frequency Response of Configuration with Three Strips

	Lengths, L (mm)	Gaps, S (mm)	x (mm)	f_{r1} (GHz)	RL_1 dB)	BW_1 (MHz)	f_{r2} (GHz)	RL_2 (dB)	BW_2 (MHz)	f_{r2}/f_{r1}	f_{r2} (GHz)	RL_2 (dB)	BW_3 (MHz)
Dual frequency	$L_1 = 33$, $L_{2(\text{fed})} = 35$, $L_3 = 33$	$S_1 = 0.2$, $S_2 = 0.2$	7	2.057	−23.07	52	2.315	−21.67	34	1.13			
	$L_1 = 34$, $L_{2(\text{fed})} = 35$, $L_3 = 34$	$S_1 = 0.2$, $S_2 = 0.2$	7	2.033	−31.24	49	2.276	−21.79	38	1.12			
	$L_1 = 35$, $L_{2(\text{fed})} = 35$, $L_3 = 35$	$S_1 = 0.2$, $S_2 = 0.2$	7	2.002	−16.99	40	2.246	−13.65	34	1.12			
	$L_1 = 36$, $L_{2(\text{fed})} = 35$, $L_3 = 36$	$S_1 = 0.2$, $S_2 = 0.2$	7	1.968	−11.75	24	2.226	−10.75	30	1.13			
Triple frequency	$L_1 = 33$, $L_{2(\text{fed})} = 35$, $L_3 = 37$	$S_1 = 0.5$, $S_2 = 0.5$	8.5	1.956	−13.18	28	2.121	−11.36	32		2.263	−20.8	36
	$L_1 = 34$, $L_{2(\text{fed})} = 35$, $L_3 = 36$	$S_1 = 1$, $S_2 = 1$	7.5	1.991	−15.05	36	2.112	−18.5	37		2.205	−18.93	42

$\varepsilon_r = 4.3$, $h = 1.59$ mm, $\tan\delta = 0.02$, $W = 15.36$ mm.

broadside as compared with the beam maxima. For the same configuration, when smaller strip is fed, the beam maxima shifts at first frequency for dual frequency operation. Also, it is observed that directivity at second frequency band is slightly more than that at first frequency band.

2.2. Configuration with Three Strips for Dual and Triple Frequency Operation

Now, the single RMSA is equally divided into three smaller elements along the width keeping the length same. The central strip is fed, while other two are gap coupled to it as shown in Figure 1(c). As the lengths of the two parasitic elements are same, these radiate at same frequency and so only two resonances are obtained in this case, even though the number of resonating elements in the system is three. If the lengths for the parasitic elements are taken different, then these will radiate at different frequencies yielding three resonances. So, both dual and triple frequency operation are possible for this configuration.

For dual frequency operation, the lengths of the two parasitic elements are kept same, so that these radiate at same frequency. Again the length of the fed element is kept same as the original RMSA, i.e., 35 mm, while the lengths of the other two identical parasitic elements are varied from smallest to largest and the performance of each configuration is investigated in detail, which is summarized in Table 2 (see results under dual frequency). The range of lengths, which yielded dual frequency response with input matching is 33–36 mm, with a maximum frequency ratio of 1.13, and bandwidth of over 30 MHz at each frequency band. This frequency ratio of 1.13 is considerably more than the maximum frequency ratio of 1.07, obtained using previous configuration with two strips. This is because now two parasitic elements radiate at same frequency, which increases the coupling, causing the loop size, in the impedance loci, to increase significantly thereby increasing the separation between two resonances as can be seen from Figure 4. Figure 4 shows the comparative input impedance loci and return loss for both the cases of configuration with 2 and 3 strips. It is seen that loop size in latter case is significantly more than that for the former.

In this symmetrical configuration, it is observed that radiation pattern at both the frequency bands is in broadside direction in both E- and H-planes. This is because at second frequency band, radiation due to parasitic elements is more dominant and as the two parasitic elements have same dimensions and coupling seen by each of them is same, each parasitic element tries to tilt the beam in opposite direction by equal amount. So the net result is that maxima remains in broadside direction as can be seen from Figure

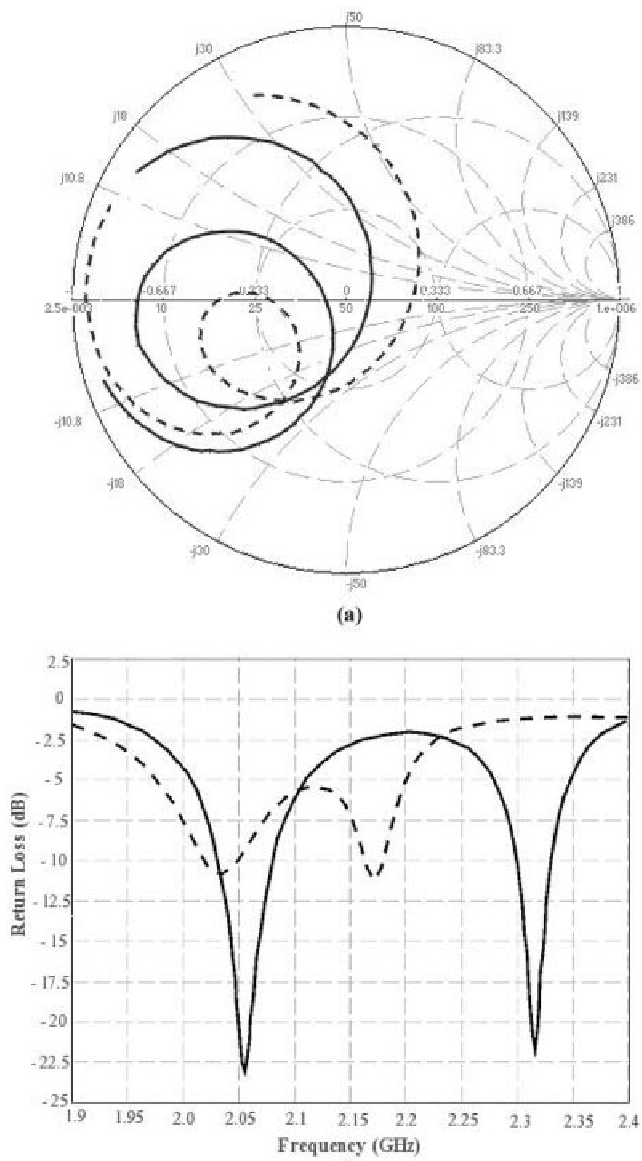

(a)

(b)

Figure 4 (a) Input impedance loci, (b) return loss plot for two and three strip configurations, showing the separation between two resonances of dual frequency operation, (- - -) configuration with two strips, (——) configuration with three strips

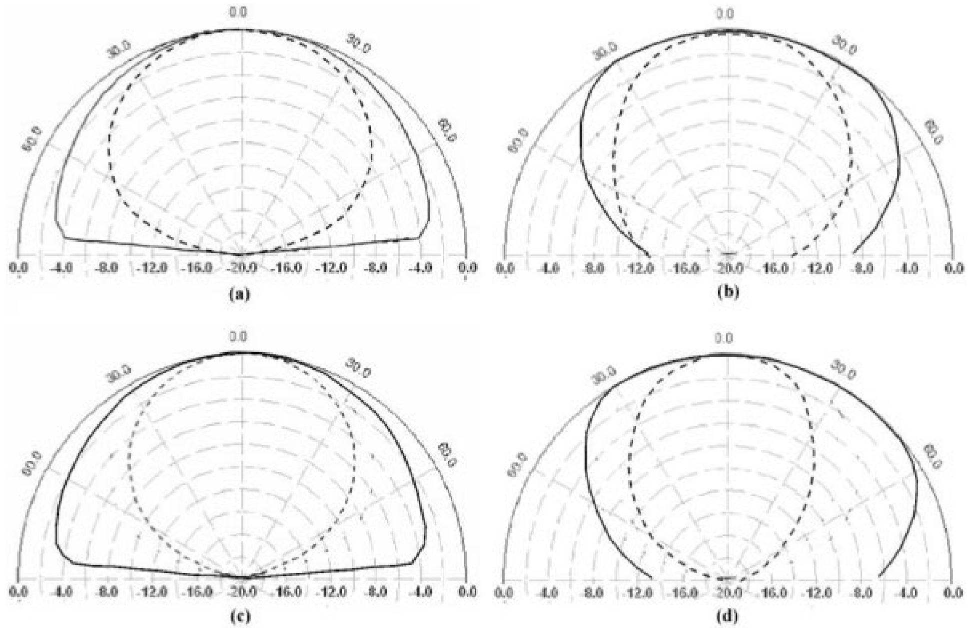

Figure 5 Radiation pattern of three strip configuration with lengths of three strips as 33, 35, and 33 mm, for dual frequency operation at two centre frequencies, (a) simulated at first frequency band, (b) measured at first frequency band, (c) simulated at second frequency band, and (d) measured at second frequency band, (——) *E*-plane, (- - -) *H*-plane

5, which shows the measured and simulated radiation patterns at two center frequencies for one of these dual band configurations. The directivity at second frequency band slightly increases. The measured and simulated results are in agreement.

For triple frequency operation, the lengths of the two parasitic elements are taken different so that these resonate at different frequencies. The length of one of the parasitic element is reduced, with respect to center patch, to increase it's resonance frequency, while the length of the other parasitic element is increased to reduce it's resonance frequency, so that separation between three resonances is maximum. Table 2(see results under triple frequency) gives the details of response of this configuration for two different cases. It is seen that in the first case, with lengths of elements as 33, 35, and 37 mm, the difference between the lengths of the individual elements is large the separation between different resonances is also large; but bandwidths at individual frequency bands is less because of improper matching. In the second case with the lengths of elements as 34, 35, and 36 mm, as the difference between lengths is small, bandwidths at individual frequency bands is large due to improved matching, but the separation between different resonances is small. As regards to radiation pattern, it is observed that at all three frequency bands, radiation pattern is in broadside in *E*-plane, but in *H*-plane the beam maxima tends to shift away from broadside at second and third frequency bands. However, at broadside, levels are only slightly less and are within 2 dB of that of the maximum levels.

Experiments are performed for the present configuration with three strips for the case of dual and triple frequency operation. The antennas are fabricated using FR4 substrate with parameters, h = 1.59 mm, $\varepsilon_r = 4.3$, and $\tan\delta = 0.02$. For dual frequency operation, the dimensions of different elements are taken as, L_1 = 33 mm, L_2 = 35 mm, and L_3 = 33 mm, with L_2 fed at x = 7 mm from center. The measured resonance frequencies are f_{r1} = 2.057 GHz and f_{r2} = 2.336 GHz, while the simulated resonance frequencies are f_{r1} = 2.057 GHz, and f_{r2} = 2.315 GHz, as can be seen from Figure 6(a) and Table 2 (see results under dual frequency). For triple frequency operation the dimensions of the different elements are taken as L_1 = 34 mm, L_2 = 35 mm, and L_3 = 36 mm, with L_2 fed at x = 7.5 mm from center. The measured resonance frequencies are f_{r1} = 1.991 GHz, f_{r2} = 2.107 GHz, and f_{r3} = 2.193 GHz, while the simulated resonance frequencies are f_{r1} = 1.991 GHz, f_{r2} = 2.112 GHz, and f_{r3} = 2.205 GHz, which can be seen from Figure 6(b) and Table 2 (see results under triple frequency).

2.3. Configuration with Four Strips for Dual and Triple Frequency Operation

Now, the single RMSA is divided into four smaller strips in similar manner, as discussed before. The configuration is shown in Figure 1(d). As there are four resonating elements in the system, which is asymmetrical about the feed point, four resonances can be obtained by suitably varying the resonance frequencies of the individual smaller strips. So, using this configuration it is possible to obtain dual, triple, and even multi frequency operation. But in this article, only dual and triple frequency operations have been investigated.

Of the four equal width splitted elements, 1st and 4th element [in Fig. 1(d)] radiate at frequencies, which are closer to each other, while the 3rd element radiates at frequency, which is closer to that of the 2nd element (i.e., fed element). So, for dual frequency operation, the lengths of the 1st and 4th element are decreased to increase their resonance frequencies, while the length of the 3rd element is increased to bring it's resonance frequency closer to that of the fed element. The length of the fed element is kept same as that of the original element, i.e., 35 mm. Table 3 (see results under dual frequency) gives the performance of this configuration for two different cases designed in this manner. Again, it is seen that in the first case as the difference between the lengths of individual elements is large, a large frequency ratio of 1.16 is obtained. The bandwidths at two frequency bands are also over 40 MHz. The bandwidths at each frequency band can be increased further if the length of the first element is slightly increased, but then the frequency ratio also decreases to 1.12. The maximum frequency ratio of 1.16 obtained in this case is more than that obtained in previous case of three elements, which is due to flexibility of controlling the length of four resonators and also because of

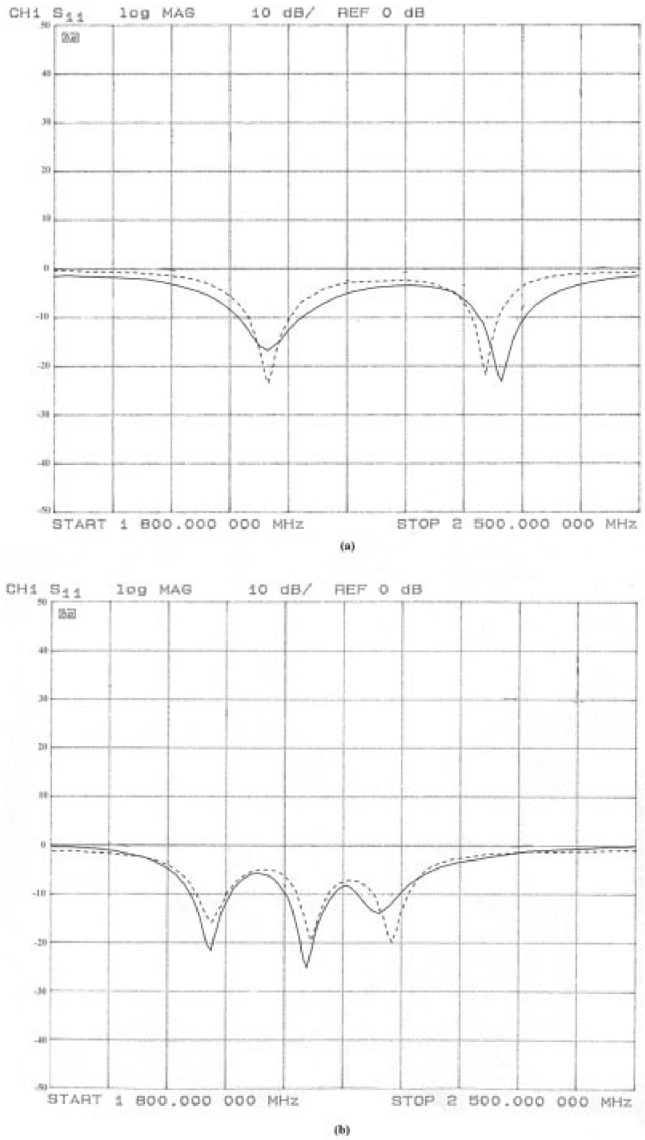

Figure 6 Comparative plot for measured and simulated S_{11} (in dB), of (a) dual frequency operation of three strip configuration with $L_1 = 33$ mm, $L_2 = 35$ mm, $L_3 = 33$ mm, (b) triple frequency operation of three strip configuration with $L_1 = 34$ mm, $L_2 = 35$ mm, $L_3 = 36$ mm, (——) measured, (- - -) simulated

increased coupling as explained before. Also, the bandwidths in two frequency bands are more and the radiation pattern also remains in broadside direction at both the frequencies.

For dual frequency operation the length of the 3rd element was increased so that it radiates at frequency closer to that of the fed element, but for triple frequency operation it's length is decreased to increase it's resonance frequency so as to increase the separation between 1st and 2nd resonance. Accordingly, Table 3 (see results under triple frequency) shows the performance of this configuration for two different cases, designed in similar manner. Again it is seen that if the difference between the lengths of the individual elements is large then the separation between the resonances is large, but bandwidths at individual frequency bands reduces. The bandwidth increases if the difference between the lengths of different elements is small, but separations between different resonances also decrease. For the second case it is seen that satisfactory triple frequency operation is obtained with a bandwidth of over 40 MHz at each frequency band. Radiation patterns, as before, are in broadside direction in *E*-plane, at all the three frequency bands. However, in *H*-plane, the beam tends to shift at second and third frequency bands but at broadside the levels are only slightly less and within 2 dB of the maximum level for all these cases.

2.4. Configuration with Five Strips for Dual and Triple Frequency Operation

Similarly, configuration with five strips is obtained as shown in Figure 1(e). In this case as there can be a maximum of five resonances, dual, triple as well as multi frequency operations are possible using this configuration. Only dual and triple frequency operations have been investigated in this article.

For dual frequency operation, the lengths of 2nd and 4th element are increased to decrease their resonance frequencies, so that they resonate at frequencies closer to that of the driven element (3rd element), while the lengths of the 1st and 5th element are decreased to increase their resonance frequencies, so that there is sufficient separation between the two frequencies of the dual frequency operation. The results are summarized in Table 4 (see results under dual frequency) for two different cases. For the case when the difference between the lengths of the different elements is large, frequency ratio of 1.19 is obtained, which is significantly more than the previous cases, but the bandwidths at two frequency bands are just over 30 MHz. When the difference between the lengths is reduced the frequency ratio reduces to 1.12. The radiation pattern at two frequency bands is again in the broadside direction, because of the symmetry of the configuration with respect to the fed patch.

Similarly, for triple frequency operation, the lengths of the 2nd and 4th element are decreased to reduce the separation between the 1st and 2nd resonances. In this case also, similar observations are made regarding the lengths of the individual elements and the separation between different resonances and

TABLE 3 Dual and Triple Frequency Response of Configuration with Four Strips

	Lengths, *L* (mm)	Gaps, *S* (mm)	*x* (mm)	f_{r1} (GHz)	RL_1 (dB)	BW_1 (MHz)	f_{r2} (GHz)	RL_2 (dB)	BW_2 (MHz)	f_{r2}/f_{r1}	f_{r3} (GHz)	RL_3 (dB)	BW_3 (MHz)
Dual frequency	$L_1 = 33$, $L_{2(fed)} = 35$, $L_3 = 37$, $L_4 = 33$	$S_1 = 1$, $S_2 = 1$, $S_3 = 3$	9	1.974	−25.22	44	2.282	−28.68	41	1.16			
	$L_1 = 34$, $L_{2(fed)} = 35$, $L_3 = 37$, $L_4 = 34$	$S_1 = 1$, $S_2 = 1$, $S_3 = 3$	11	1.977	−21.67	57	2.210	−16.62	53	1.12			
Triple frequency	$L_1 = 32$, $L_{2(fed)} = 35$, $L_3 = 35$, $L_4 = 32$	$S_1 = 1$, $S_2 = 1$, $S_3 = 3$	9	2.05	−11.24	48	2.163	−12.83	46		2.345	−12.48	23
	$L_1 = 33$, $L_{2(fed)} = 35$, $L_3 = 35$, $L_4 = 33$	$S_1 = 1$, $S_2 = 1$, $S_3 = 3$	9	2.044	−12.08	56	2.155	−16.79	55		2.284	−33.07	42

$\varepsilon_r = 4.3$, $h = 1.59$ mm, $\tan \delta = 0.02$, $W = 11.52$ mm.

TABLE 4 Dual and Triple Frequency Response of Configuration with Five Strips

	Lengths, L (mm)	Gaps, S (mm)	x (mm)	f_{r1} (GHz)	RL_1 (dB)	BW_1 (MHz)	f_{r2} (GHz)	RL_2 (dB)	BW_2 (MHz)	f_{r2}/f_{r1}	f_{r3} (GHz)	RL_3 (dB)	BW_3 (MHz)
Double frequency	$L_1 = 33$, $L_2 = 37$, $L_{3(fed)} = 35$, $L_4 = 37$, $L_5 = 33$	$S_1 = 1$, $S_2 = 0.2$, $S_3 = 0.2$, $S_4 = 1$	6.5	1.954	−28.99	30	2.323	−28.14	35	1.19			
	$L_1 = 34$, $L_2 = 36$, $L_{3(fed)} = 35$, $L_4 = 36$, $L_5 = 34$	$S_1 = 2.3$, $S_2 = 1.2$, $S_3 = 1.2$, $S_4 = 2.3$	7	1.993	−30.83	36	2.241	−17.83	39	1.12			
Triple frequency	$L_1 = 33$, $L_2 = 34$, $L_{3(fed)} = 35$, $L_4 = 34$, $L_5 = 33$	$S_1 = 2.3$, $S_2 = 1.2$, $S_3 = 2.3$, $S_4 = 1.2$	5	2.066	−23.98	35	2.262	−16.41	24		2.35	−42.77	19
	$L_1 = 34$, $L_2 = 34$, $L_{3(fed)} = 35$, $L_4 = 34$, $L_5 = 34$	$S_1 = 2.3$, $S_2 = 1.2$, $S_3 = 2.3$, $S_4 = 1.2$	5	2.058	−17.22	31	2.219	−19.72	22		2.338	−13.65	18

$\varepsilon_r = 4.3$, $h = 1.59$ mm, $\tan \delta = 0.02$, $W = 9.21$ mm.

the bandwidth. However, even though separation between the resonances is more for this configuration than previous cases, but it observed that bandwidths in different frequency bands are just over 18 MHz, which are significantly less than the previous case. This is because of improper matching. Bandwidth at each frequency can be improved by reducing the separation between each resonances.

3. CONCLUSION

An RMSA is splitted into smaller elements along the width. Of these smaller elements, one of the element is fed using coaxial probe while others are coupled to it's nonradiating edge. The lengths of the individual elements are then varied to increase the separation between different resonances to obtain dual and triple frequency operation. Likewise, configurations consisting a maximum till five smaller strips have been investigated and following observations can be made. When the difference between the lengths of the different elements is large then the separation between the resonances is more yielding larger frequency ratio, but the bandwidths at the individual frequency bands is less as matching is not optimum. Frequency ratio increases with increase in number of elements in the system. With two elements the maximum dual frequency ratio obtained is only 1.07, but for configuration with five strips a maximum frequency ratio of 1.19 has been obtained. Also, with increase in number of elements, the radiation characteristics of the configuration also improve. As all these configurations are obtained by splitting a RMSA, and lengths are changed slightly, the configuration is compact. These configurations can be used for applications where dual frequency ratio required is small to moderate. For higher frequency ratio the patch should be splitted further into more number of equal width strips and optimize the lengths.

REFERENCES

1. K.P. Ray and G. Kumar, Multi-frequency and broadband hybrid-coupled circular microstrip antennas, Electon Lett 33 (1997), 437–438.
2. K.P. Ray and G. Kumar, Compact gap-coupled shorted 90° sectoral microstrip antennas for broadband and dual band operations, Microwave Opt Techol Lett 26 (2000), 143–145.
3. G. Kumar and K.P. Ray, Broadband microstrip antennas, Artech House, Boston, 2003.
4. K.P. Ray, V. Sevani, and S. Kakatkar, Compact broadband gap coupled rectangular microstrip antennas, Microwave Opt Technol Lett 48 (2006), 2384–2389.
5. IE3D 9.21, Zeland Software Inc., Fremont, CA, 2002.
6. G. Kumar and K.C. Gupta, Broadband microstrip antennas using additional resonators gap coupled to the radiating edges, IEEE Trans Antennas Propag 32 (1986), 1375–1379.
7. G. Kumar and K.C. Gupta, Non-radiating edges and four edges gap coupled with multiple resonator, broadband microstrip antennas, IEEE Trans Antennas Propag 33 (1985), 173–178.

DESIGN OF A V-SHAPED SURFACE-MOUNTED MONOPOLE ARRAY ANTENNA FOR DCS/PCS OPERATIONS

Jean-Marie Floc'h and Hatem Rmili
IETR, UMR CNRS 6164, 20 Avenue Buttes des Coësmes, 35043 Rennes, France

Received 23 October 2006

ABSTRACT: *In this paper, a surface-mountable, reconfigurable monopole antenna was designed for array antenna operations in the DCS-1800 and PCS-1900 bands. First, the elementary structure was obtained by folding a metallic strip into a V-shape, and then soldered to a 50-Ω microstrip feed line printed on a metallized substrate. For the optimized structure, an impedance bandwidth of 22.7%, corresponding to the frequency range 1560–1960 MHz, was obtained. Measured radiation patterns are similar to that of a monopole antenna, and the maximum measured gain is about 1.8 dBi at 1.6 GHz. Next, this elementary antenna was used for realization of both linear- and planar-array antennas. The linear-array shows a dual and wideband behavior with good impedance matching and asymmetric radiation patterns, whereas the planar-array presents a unique resonant band with moderate adaptation and symmetric radiation patterns. The measured gain for the two arrays is about 5 dBi.* © 2007 Wiley Periodicals, Inc. Microwave Opt Technol Lett 49: 1486–1491, 2007; Published online in Wiley InterScience (www.interscience.wiley.com). DOI 10.1002/mop.22437

Key words: *monopole antenna; surface-mountable antenna; array antenna; wireless communication*

1. INTRODUCTION

Monopole antennas have found widespread applications, especially with the rapid progress in wireless communications. Various types of monopole antennas have been studied to meet the increasing trend for wideband/multiband antennas. Planar monopole antenna has attractive advantages of simple structure and omnidirec-